ULTRASONOGRAPHY

Portable high-intensity focused ultrasound system with 3D electronic steering, real-time cavitation monitoring, and 3D image reconstruction algorithms: a preclinical study in pigs

ORIGINAL ARTICLE

http://dx.doi.org/10.14366/usg.14008
pISSN: 2288-5919 • eISSN: 2288-5943
Ultrasonography 2014;33:191-199

Jin Woo Choi, Jae Young Lee, Eui Jin Hwang, Inpyeong Hwang, Sungmin Woo, Chang Joo Lee, Eun-Joo Park, Byung Ihn Choi

Department of Radiology and Institute of Radiation Medicine, Seoul National University Hospital, Seoul, Korea

Purpose: The aim of this study was to evaluate the safety and accuracy of a new portable ultrasonography-guided high-intensity focused ultrasound (USg-HIFU) system with a 3-dimensional (3D) electronic steering transducer, a simultaneous ablation and imaging module, real-time cavitation monitoring, and 3D image reconstruction algorithms.

Methods: To address the accuracy of the transducer, hydrophones in a water chamber were used to assess the generation of sonic fields. An animal study was also performed in five pigs by ablating *in vivo* thighs by single-point sonication (n=10) or volume sonication (n=10) and *ex vivo* kidneys by single-point sonication (n=10). Histological and statistical analyses were performed.

Results: In the hydrophone study, peak voltages were detected within 1.0 mm from the targets on the y- and z-axes and within 2.0-mm intervals along the x-axis (z-axis, direction of ultrasound propagation; y- and x-axes, perpendicular to the direction of ultrasound propagation). Twenty-nine of 30 HIFU sessions successfully created ablations at the target. The *in vivo* porcine thigh study showed only a small discrepancy (width, 0.5–1.1 mm; length, 3.0 mm) between the planning ultrasonograms and the pathological specimens. Inordinate thermal damage was not observed in the adjacent tissues or sonic pathways in the *in vivo* thigh and *ex vivo* kidney studies.

Conclusion: Our study suggests that this new USg-HIFU system may be a safe and accurate technique for ablating soft tissues and encapsulated organs.

Keywords: High-intensity focused ultrasound ablation; Ablation techniques; Animal research; Equipment and supplies

Received: January 23, 2014
Revised: March 24, 2014
Accepted: March 26, 2014

Correspondence to:
Jae Young Lee, MD, Department of Radiology, Seoul National University Hospital, 101 Daehak-ro, Jongno-gu, Seoul 110-744, Korea

Tel. +82-2-2072-3073
Fax. +82-2-743-6385
E-mail: leejy4u@snu.ac.kr

How to cite this article:
Choi JW, Lee JY, Hwang EJ, Hwang I, Woo S, Lee CJ, et al. Portable high-intensity focused ultrasound system with 3D electronic steering, real-time cavitation monitoring, and 3D image reconstruction algorithms: a preclinical study in pigs. Ultrasonography. 2014 Jul;33(3):191-199.

Introduction

High-intensity focused ultrasound (HIFU) is a promising technology that has shown promising results in diverse clinical and preclinical studies [1–6]. This technique has attracted special attention not only as a tumor ablation method but also as a gene delivery, drug delivery, and immunotherapy modality [7,8].

In an effort to improve treatment efficacy and safety, current HIFU machines are operated in combination with a few different image-guiding systems. Therefore, on the basis of the combined imaging modalities, the HIFU system can be divided into magnetic resonance-guided HIFU (MRg-HIFU) and ultrasonography-guided HIFU (USg-HIFU) [1]. In particular, MRg-HIFU is advantageous for identifying the target and adjacent structures with a high contrast resolution and to monitor the temperature with magnetic resonance (MR) thermometry techniques, which makes the system feasible for treating uterine fibroids and various brain diseases in real clinical practice [1,9–11]. In contrast, USg-HIFU has potential strengths in the "real-time" monitoring of the targets in terms of acoustic cavitation, as well as structural changes [12–14]. These potential advantages may be particularly beneficial to the ablation of moving structures such as the liver and kidneys, compared with the MRg-HIFU system. In addition, ideally, USg-HIFU can provide operators with more flexibility because it does not require a large gantry, which is indispensable in MRg-HIFU [3].

Despite the aforementioned potential strengths, unfortunately, USg-HIFU has not been widely used in clinical practice mainly because the potential strengths of USg-HIFU have not been actualized sufficiently to overcome its weaknesses of providing less accuracy in planning and post-ablation assessment, compared with MRg-HIFU [3,15]. However, with recent advances in ultrasound (US) transducers and image processing techniques, many trials to maximize the strengths and minimize the weaknesses of USg-HIFU are being performed on an ongoing basis, for instance, by adopting 3-dimensional (3D) electronic steering transducers and real-time 3D ultrasonography [1,16,17]. In addition, new USg-HIFU systems allow portability in adopting compact HIFU devices with high-powered equipment. Furthermore, a diagnostic ultrasonography system and HIFU are synchronized, which provides real-time ultrasonography during ablation without the interference phenomenon [18,19].

Considering the above-mentioned advances in US technologies, we believe that the strengths of up-to-date USg-HIFU are worth revisiting. Therefore, we conducted a hydrophone study and preclinical *in vivo* and *ex vivo* studies to address the safety and accuracy of a new portable USg-HIFU unit equipped with a 3D electronic steering transducer, a simultaneous ablation and imaging module, real-time cavitation monitoring, and 3D image reconstruction algorithms.

Materials and Methods

The investigational HIFU system for this study was provided by Alpinion Medical Systems (Seoul, Korea). The authors had complete control of the experimental data, which were unbiased by the industry.

Animals

This study was approved by our Institutional Animal Care and Use Committee (IACUC protocol number 13-0001), and performed in accordance with the institutional guidelines. Five male pigs that weighed 50–60 kg were used in our study. For the *in vivo* study, the pigs were starved 12 hours prior to the HIFU ablation. Each animal was sedated with an intramuscular injection of zolazepam (5 mg/kg, Zoletil; Virbac, Carroscedex, France) and xylazine (10 mg/kg, Rompun; Bayer-Schering Pharma, Berlin, Germany), and the animals were then intubated and ventilated during the procedures. Anesthesia was maintained by the inhalation of 1%–3% isoflurane in pure oxygen gas. To facilitate US propagation through the skin, the pigs underwent the shaving and subsequent waxing of their bilateral thighs and flanks prior to the procedures. During the entire HIFU procedures, the animals' vital signs, including pulse rate, electrocardiogram, and temperatures, were carefully monitored.

USg-HIFU System

The USg-HIFU device (ALPIUS; Alpinion Medical Systems, Seoul, Korea) used in our study is 1.8 m, 1.2 m, and 1.6 m in length, width, and height, respectively (Fig. 1). The four wheels installed under the

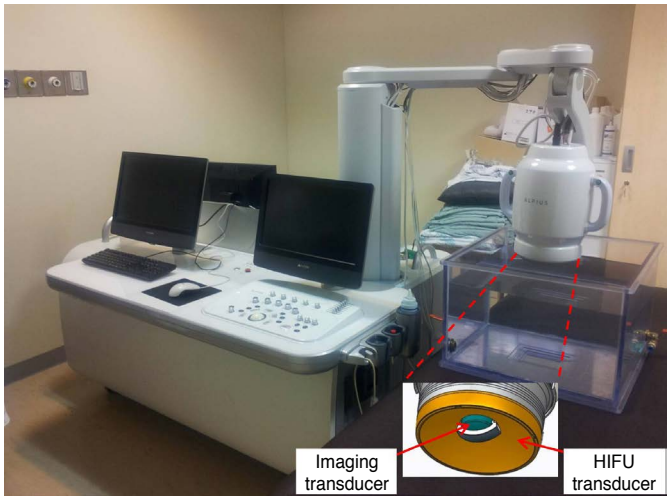

Fig. 1. A photograph showing the ultrasonography-guided high-intensity focused ultrasound (HIFU) system used in this study.

main body make the device portable. The system includes an HIFU transducer with a focal length of 9 cm driven at its fundamental frequency of 1 MHz. This system had a phased-array 256-channel transducer (radius of curvature, 9 cm; aperture size, 15 cm), which has a steering range along the z-axis of 40 mm and along the x- and y-axes of 24 mm (z-axis, direction of US propagation; y- and x-axes, perpendicular to the direction of US propagation). Therefore, the system can perform volumetric ablation by electronically steering the focal spots in a 3D space, without repositioning the transducer. The natural focal size of the transducer is 1.5 mm×1.5 mm×8 mm at −6 dB. The ultrasonic power measured using a radiation-force balance system varies from 1 W to 1 kW. During ablation, the transducer can be cooled using degassed water at 9°C–15°C.

In terms of the imaging guidance, a 3.5-MHz ultrasonography transducer is placed at the center of the HIFU transducer for the planning and treatment monitoring. As the image transducer rotates, it provides the 3D volume data reconstructed from 2D images, which can be used for ablation planning. During the procedure, ablation was supervised through the interleaving/synchronization control between the HIFU ablation and the imaging modules. In addition, this system has four passive cavitation detection (PCD) sensors installed on the US radiation surface of the HIFU transducer. During the procedure, the occurrence of excessive microbubbles can be monitored by a preinstalled system that archives the acoustic signals obtained from the PCD sensors [20–22].

Accuracy Study of Acoustic Steering Using Hydrophones

To address the targeting accuracy of the transducer, hydrophones (AST3-L; ONDA Co., Sunnyvale, CA, USA) in a water chamber assessed the sonic field generation during HIFU ablation (Fig. 2). On

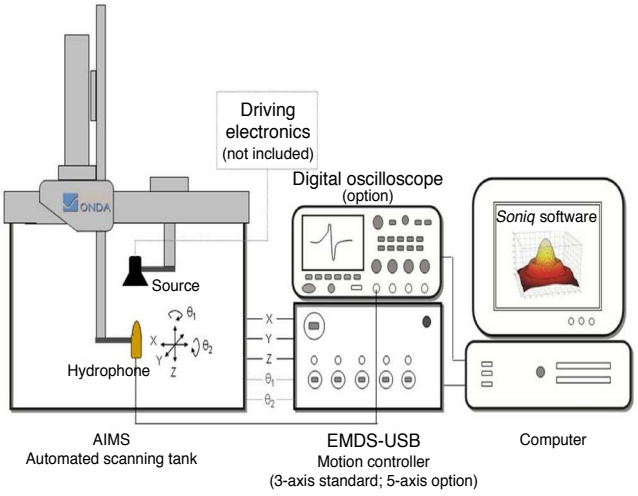

A

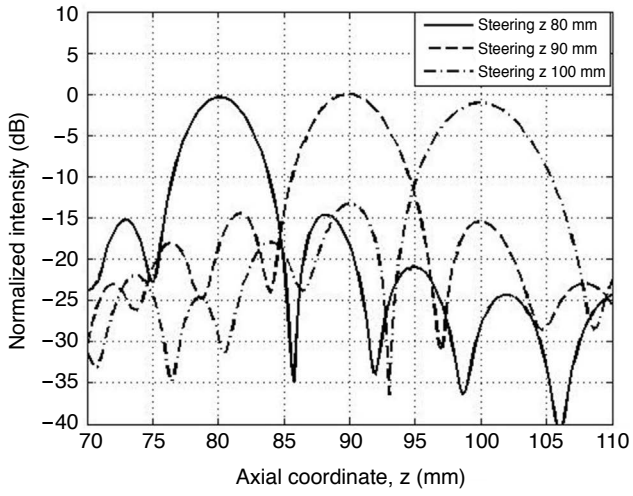

B

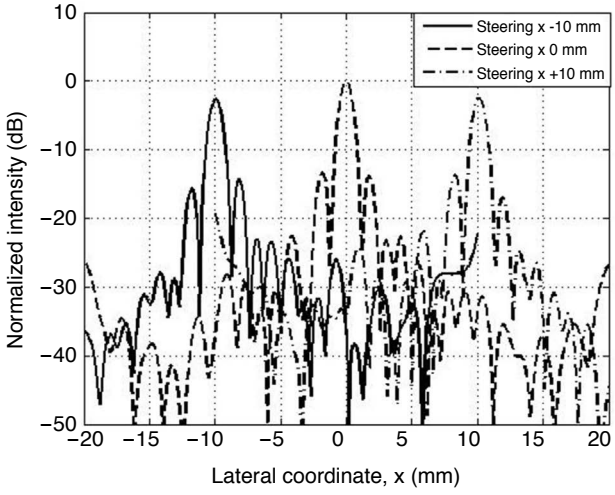

C

Fig. 2. An *ex vivo* study to evaluate the accuracy of our transducer. AIMS, acoustic intensity measurement system; EMDS-USB, electronic motor drive system-universal serial bus.
A. Schematic representation depicting the phased array transducer (high-intensity focused ultrasound source) and a hydrophone fixed in a water chamber, which archived the peak voltages in the x-, y-, and z-coordinates. B, C. Plots showing the peak voltage measurements in the axial (z-axis) and lateral (x-axis) coordinates.

the premise that the trajectory of sonication in the neutral status is along the z-axis, 10-mm beam steering on the x- and y-axes (with targets having depths of 70 mm, 90 mm, and 110 mm) was tested, using the phased-array HIFU transducer. In particular, 15 imaginary targets with different x-, y-, and z-coordinates were aimed: (0, 0, 70), (−10, 0, 70), (10, 0, 70), (0, −10, 70), (0, 10, 70), (0, 0, 90), (−10, 0, 90), (10, 0, 90), (0, −10, 90), (0, 10, 90), (0, 0, 110), (−10, 0, 110), (10, 0, 110), (0, −10, 110), and (0, 10, 110). The phased-array transducer, fixed in the water chamber, changed the x- and y-axes using beam steering. After each experiment, the x-, y-, and z-coordinates of the peak voltage (recorded in the hydrophones) were archived to evaluate the transducer accuracy. The peak voltage was measured five times for each target point.

Animal Study

The animal studies were performed with *in vivo* thighs and *ex vivo* kidneys of five pigs. On the HIFU bed, volumetric ultrasonograms were obtained using an imaging transducer embedded in the HIFU machine for planning the ablation. Based on the 3D plan and preset protocols, the pigs were extracorporeally ablated for the imaginary targets, with two "single-point sonication" modes in the left thigh and two "volume sonication" modes in the right thigh (Table 1). During the procedures, echogenic changes in the target and the occurrence of excessive acoustic cavitation were monitored in real-time. If inordinate cavitation was detected during the procedure, the ablation was discontinued to minimize adverse effects. The animals were euthanized within 3 hours after the procedure by using an intravenous injection of potassium chloride (2 ampoules/pig, 20 mL/ampoule, JW Pharmaceutical, Seoul, Korea), and their thighs were sampled for the histological analyses.

Subsequently, studies using explants were conducted to evaluate the safety of HIFU ablation in a deep-seated, encapsulated organ, overlaid by other tissues with various sonic interfaces. After euthanasia of the animals, the pigs' kidneys along with adjacent retroperitoneal fat tissues, abdominal wall muscles, subcutaneous tissues, and skin were isolated. A thin-wire thermocouple (75 μm, Omega Engineering, Stamford, CT, USA) was inserted in either end of the kidney, away from the ablation zone, to monitor the potential thermal effect of the untargeted area in the kidney. Afterwards, the kidneys were immobilized on a gel pad in a container located at the center of a degassed water tank, and all the samples were maintained at 35°C–37°C during the entire experiment, to simulate the intra-abdominal conditions (Fig. 3). The HIFU procedure was conducted to ablate the renal parenchyma under the guidance of ultrasonography (Table 1).

Histological Analysis

Prior to tissue preparation, changes in the skin, if any, were inspected to detect undesirable skin damage. The thigh specimens, including the entire muscle layer and the overlying skin and subcutaneous fat tissues combined were sampled to be 22 cm×18 cm in area and 8 cm in thickness. The tissue blocks were immediately immersed in 1.5 L of normal saline at 4°C. To fix the specimens, three serial

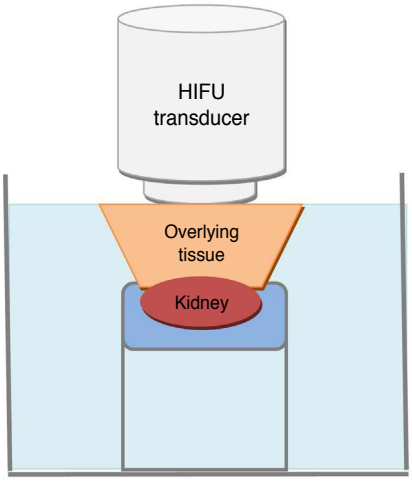

Fig. 3. **Schematic representation of the experiment using isolated kidney samples.** HIFU, high-intensity focused ultrasound.

Table 1. **High-intensity focused ultrasound ablation parameters considered in our study**

Mode	Acoustic power (W)	No. of ablation points	Exposure time per point (sec)	Duty cycle (%)	Inter-point movement time (sec)	Total procedure time (sec)	Target depth from the skin (mm)
In vivo study (thigh muscles)							
Single-point sonication	80	7	4	80	0.5	31	30
	96	7	4	80	0.5	31	30
Volume sonication	80	19	4	80	0.5	85	40
	72	37	4	80	0.5	166	40
Ex vivo study (kidneys)							
Single-point sonication	150	7	10	80	0.5	73	30

sections (dimensions of each section: 22 cm×6 cm×8 cm) parallel to the axis of the sonic pathway were obtained and embedded in 10% buffered formalin for 4 days. Subsequently, serial sections parallel to the previous section having a thickness of 4 mm were acquired from the fixed tissues. From these specimens, undesirable thermal damage in the sonic pathways and the size of the ablation zone were evaluated. For further evaluation, the target lesions and the surrounding healthy tissues were sampled; they had a thickness of 4 μm and were stained with hematoxylin-eosin-saffron. The kidney specimens were prepared in the same manner and were serially sliced to have a thickness of 4 mm. From these specimens, undesirable thermal damage in the sonic pathways was evaluated.

Statistical Analysis

The discrepancy in the ablation sizes on the planning US images and gross specimens were evaluated using the Bland-Altman method [23]. A P-value of less than 0.05 was determined to indicate statistical significance. Statistical analyses were performed using MedCalc ver. 12.7 (MedCalc Software, Ostend, Belgium).

Results

According to the accuracy study of acoustic steering using hydrophones, peak voltages were detected within 1.0 mm of the imaginary targets on the y- and z-axes, and within 2.0-mm intervals along the x-axis, for all targets (Fig. 2).

In the porcine study, 29 of 30 HIFU sessions (96.7%), including 19 targets in *in vivo* thighs and 10 targets in *ex vivo* kidneys, successfully created ablation zones. In the remaining HIFU session targeting the thigh, excessive acoustic cavitation was observed in real-time; therefore, the procedure was terminated earlier than originally planned. In this session, B-mode ultrasonography also demonstrated diffuse hyperechoic changes in and around the target. Therefore, this case was used only for safety evaluations and was excluded from the accuracy analyses.

In terms of safety, ultrasonograms acquired simultaneously during each HIFU session demonstrated that ablation occurred according to the plans drawn on the 3D ultrasonograms. Concordantly, gross and histological examinations revealed that none of the 30 specimens, including both thighs and kidneys, received inordinate tissue injury in the sonic pathways. In the kidney studies, interfaces between different tissues were also intact in all specimens. According to the histological analyses, healthy tissues beyond the target demonstrated normal structures, in contrast with disrupted architecture in the targets (Fig. 4). In addition, there was a temperature increase of less than 2°C in all kidneys.

With respect to the accuracy of the *in vivo* study, variable targets 6.0–11.0 mm in depth (z-axis) and 7.0–8.0 mm in width (x- and y-axes) were aimed with single-point sonication modes (80 W, 96 W). Consequently, ablation volumes were created with a length of 9.8–13.6 mm and a width of 4.9–7.7 mm (Table 2). With respect to the volume sonication modes (72 W, 80 W), the targets were planned to be 13.8–22.0 mm in length and 13.9–19.8 mm in width. As a result, ablation volumes with a length of 14.0–28.9 mm and a width of 9.5–24.0 mm were obtained (Table 2).

According to the Bland-Altman plots, the actual ablation volume

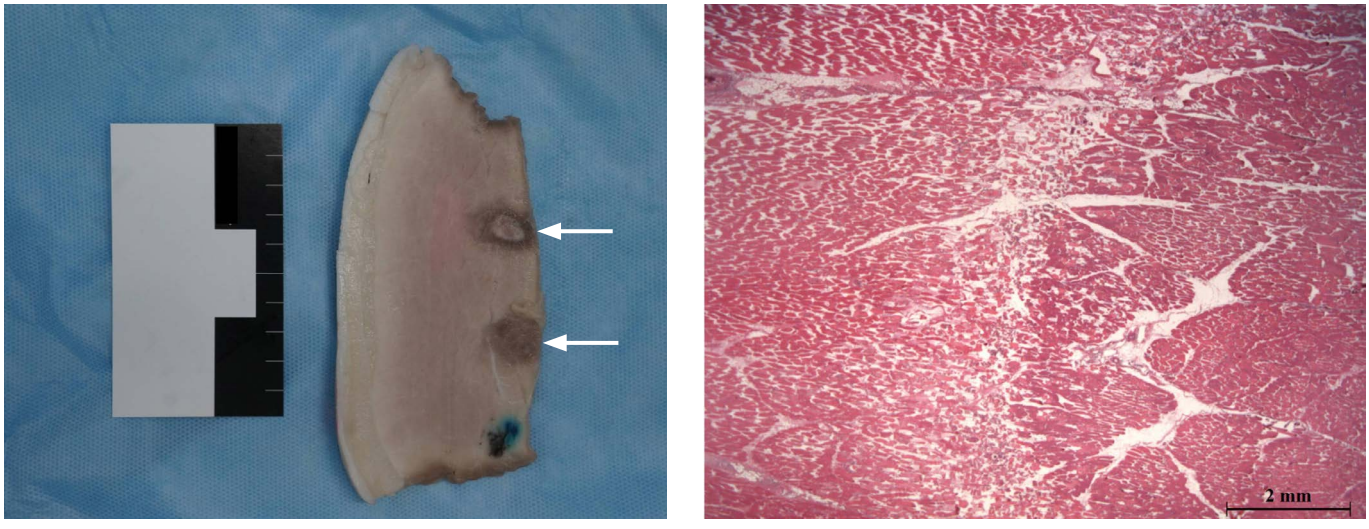

A B

Fig. 4. Histological specimens of the *in vivo* study targeting the thigh muscles of a pig.
A. Photograph showing two ablated targets (arrows) formed by the volume sonication mode in the thigh muscle. B. Microscopic image (hemotoxylin-eosin-saffron staining, ×12.5) showing normal area on the left, ablated area on the right, and transitional zone in the middle.

in the single-point sonication mode was 3.0±4.5 mm (mean±SD) larger in length and 1.1±1.9 mm smaller in width than that of the preprocedural planning (Fig. 5). The actual ablation achieved in the volume sonication mode was 3.0±1.6 mm larger in length and 0.5±8.8 mm smaller in width, compared with the planning ultrasonograms (Fig. 6).

Discussion

This new portable USg-HIFU system equipped with a state-of-

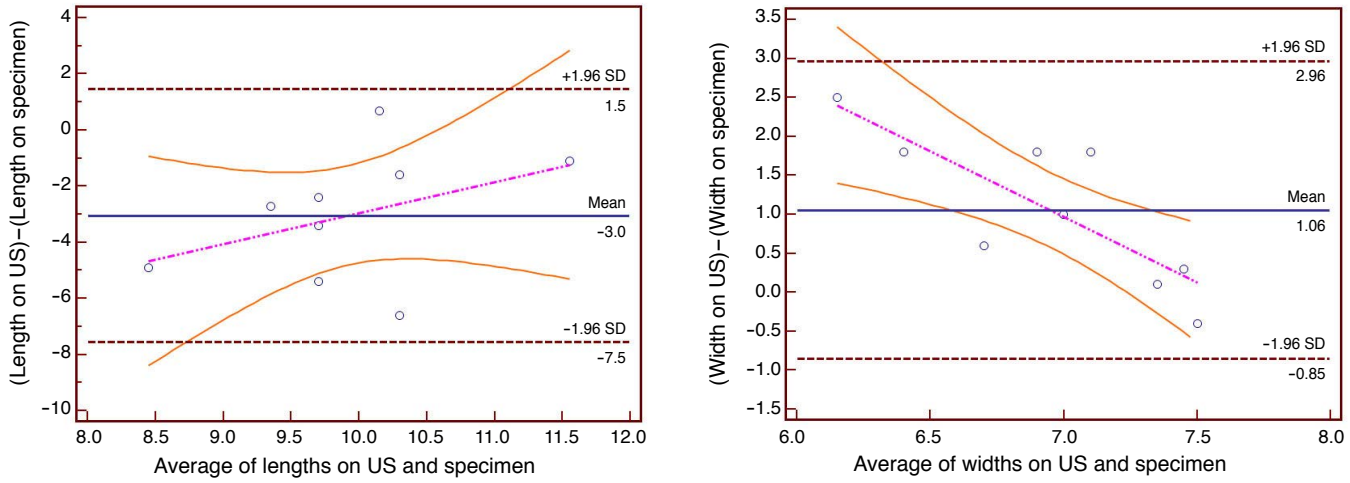

A B

Fig. 5. Bland-Altman plots showing the accuracy of the single-point sonication mode. The pink and orange lines denote the regression line and its 95% confidence interval. US, ultrasonography.
A. In terms of the length, the histological specimens reveal a 3.0±4.5 mm (mean±SD) larger ablation zone than the planning ultrasonograms. There is a slight tendency for the shallower targets (smaller depths) to create larger discrepancies along the z-axis. B. In terms of the width, the histological specimens reveal a 1.1±1.9 mm smaller ablation zone than the planning images.

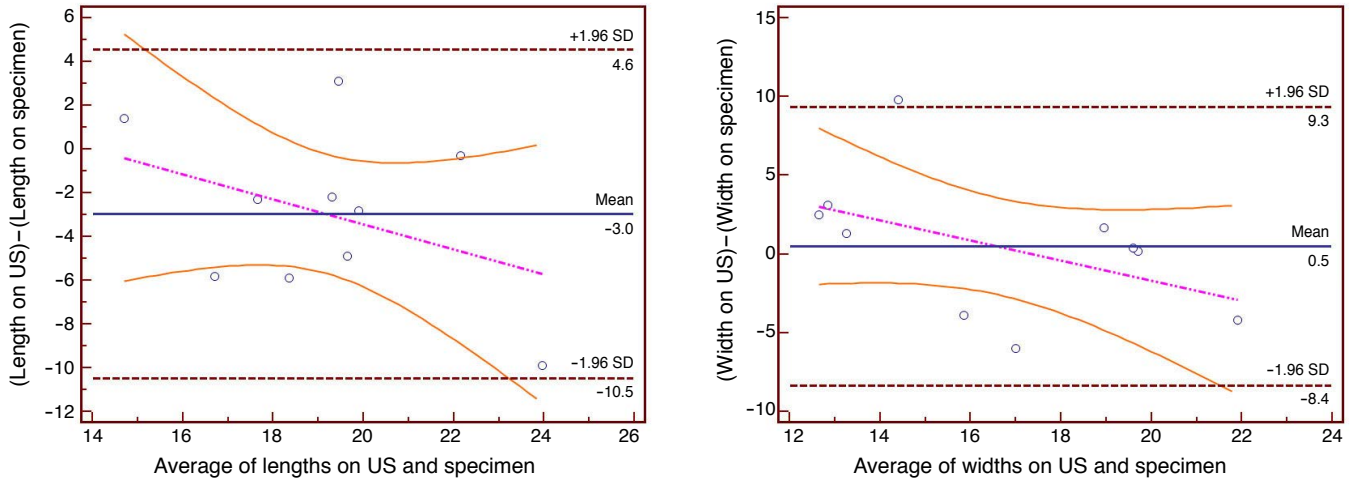

A B

Fig. 6. Bland-Altman plots showing the accuracy of the volume sonication mode. The pink and orange lines denote the regression line and its 95% confidence interval US, ultrasonography.
A. In terms of the length, the histological specimens reveal a 3.0±1.6 mm (mean±SD) larger ablation zone than the planning ultrasonograms. There is a slight tendency for shallower targets (smaller depths) to create larger discrepancies along the z-axis. B. In terms of the width, the histological specimens reveal a 0.5±8.8 mm smaller ablation zone than the planning images.

Table 2. Comparison of the ablation size estimated on the planning ultrasonograms and specimens

Mode	Pig ID	Size in the ultrasonograms (A)		Size on gross pathology (B)	
		Length (mm)	Width (mm)	Length (mm)	Width (mm)
Single-point sonication (80 W)	1	8.0	7.4	10.7	7.3
	2	7.0	7.3	12.4	5.5
	3	7.0	7.3	13.6	7.7
	4	6.0	7.0	10.9	6.4
	5	8.0	7.4	11.4	4.9
Single-point sonication (96 W)	1[a]	–	–	–	–
	2	10.5	8.0	9.8	6.2
	3	9.5	7.6	11.1	7.3
	4	8.5	7.5	10.9	6.5
	5	11.0	7.8	12.1	6.0
Volume sonication (72 W)	1	19.0	19.8	28.9	19.6
	2	16.5	19.3	18.8	9.5
	3	21.0	19.8	17.9	18.1
	4	22.0	19.8	22.3	19.4
	5	18.5	19.8	21.3	24.0
Volume sonication (80 W)	1	15.4	13.9	14.0	11.4
	2	13.8	13.9	19.6	12.6
	3	18.2	14.4	20.4	11.3
	4	15.4	13.9	21.3	17.8
	5	17.2	14.0	22.1	20.0

[a] These data were excluded from analysis because the high-intensity focused ultrasound was terminated early, based on the results of the acoustic cavitation monitoring.

the art transducer enabling 3D electronic steering and real-time cavitation monitoring and a 3D reconstruction imaging algorithm demonstrated high safety and high accuracy, that is, close similarity between the planning and the real ablated lesions. Compared with an MRg-HIFU study with a similar experimental design [9], the small discrepancy (mean width, 0.5–1.1 mm; mean length, 3.0 mm) between the planning ultrasonograms and the pathological specimens in our study suggests at least a comparable accuracy between the MRg-HIFU and the USg-HIFU systems. The high accuracy of this USg-HIFU system might stem from the precise preprocedural planning of the 3D images and the excellent control unit, which facilitated accurate predictions of the created ablation size. The 3D images can compensate for an erroneous perception of the target (depending on the position of the transducer and the target) and may provide objective and reproducible volume data to the operators. For these reasons, this image reconstruction technique has already been widely used in various clinical fields [24,25].

This USg-HIFU system demonstrated satisfactory safety in that none of the 30 specimens received inordinate tissue injury in the sonic pathways. In contrast with MRg-HIFU, USg-HIFU can reveal real-time structural changes in the target and real-time spatial relationships between the targets and the transducers in the sonic pathway. Furthermore, recently developed algorithms facilitate a reliable assessment of real-time cavitation creation during ablation [20–22]. These methods are helpful in determining the optimal projection and in avoiding potentially dangerous sonication. Concordantly, our results showed precise ablation of the targets without any unintended tissue damage. In particular, the real-time cavitation monitoring system allowed early termination of a case that was considered excessively damaged. Our results also demonstrate that this USg-HIFU technique may be safe for ablating deep-seated, encapsulated organs such as the kidneys. Because many ablative targets such as uterine fibroids, renal cell carcinomas, and liver tumors are deep-seated and located within encapsulated organs, these results suggest the clinical applicability of our USg-HIFU system.

Moreover, the portability of our device may provide new clinical applications. Compared with many current USg-HIFU and MRg-HIFU devices fixed in a dedicated room, this USg-HIFU system can be moved to and installed at the bedside. In other words, this system may yield superior comfort for patients, provide operators greater accessibility to patients, and make better use of hospital space. Furthermore, given that the MRg-HIFU system limits the use of many metallic medical devices in the operating room, the USg-HIFU system appears to offer greater flexibility for combination with other medical procedures or advanced monitoring equipment.

There are a few limitations to our study. First, we were unable to directly compare the performance of this USg-HIFU with that of MRg-HIFU. However, the high accuracy of this USg-HIFU system appears to be acceptable to clinicians. Furthermore, our results are apparently comparable with those of a MRg-HIFU study with a similar experimental design [9]. Second, the sample size in our study is quite small. However, we utilized the 5 animals using various methods and were thus able to conduct 30 ablation sessions. Considering that this investigation was a preclinical feasibility study, our study design appears to be acceptable with respect to scientific rigor and animal welfare. Third, we did not identify the therapeutic effect of our system on mobile structures such as the liver. However, it is expected that this USg-HIFU system, which showed excellent accuracy in static tissues, may be applicable to mobile organs, along with adequate gating and monitoring systems. Fourth, the accuracy of targeting the sonication spot was not evaluated. Since the accurate localization of the target is critical for safe HIFU treatments, it should be fully evaluated in future studies. Additionally, *in vivo*

kidney experiments should be conducted in the next step to evaluate the suitability of this USg-HIFU system for safe HIFU treatment.

In conclusion, this study demonstrated the high safety and accuracy of a new USg-HIFU system that was equipped with a compact and high-powered electronic steering transducer, a simultaneous ablation and imaging module, and real-time cavitation monitoring under the guidance of a 3D, real-time, and portable ultrasonography device. Compared with the MRg-HIFU, this USg-HIFU system might provide more flexibility and comparable accuracy and safety in many applications.

ORCID: Jin Woo Choi: http://orcid.org/0000-0002-6639-8002; Jae Young Lee: http://orcid.org/0000-0001-6946-6042; Eui Jin Hwang: http://orcid.org/0000-0002-3697-5542; Inpyeong Hwang: http://orcid.org/0000-0002-1291-8973; Sungmin Woo: http://orcid.org/0000-0001-8459-8369; Chang Joo Lee: http://orcid.org/0000-0003-2556-5721; Eun-Joo Park: http://orcid.org/0000-0003-2556-6257; Byung Ihn Choi: http://orcid.org/0000-0002-5613-1881

Conflict of Interest

The investigational HIFU system for this study was provided by Alpinion Medical Systems (Seoul, Korea). The authors had complete control of the experimental data, which were unbiased by the industry.

Acknowledgments

This work was supported by the R&D program of MKE/KEIT (10033702, Ultra High-Speed Parallel Beamforming & Signal Processing).

References

1. Malietzis G, Monzon L, Hand J, Wasan H, Leen E, Abel M, et al. High-intensity focused ultrasound: advances in technology and experimental trials support enhanced utility of focused ultrasound surgery in oncology. Br J Radiol 2013;86:20130044.
2. Lee JY, Choi BI, Ryu JK, Kim YT, Hwang JH, Kim SH, et al. Concurrent chemotherapy and pulsed high-intensity focused ultrasound therapy for the treatment of unresectable pancreatic cancer: initial experiences. Korean J Radiol 2011;12:176-186.
3. Orsi F, Arnone P, Chen W, Zhang L. High intensity focused ultrasound ablation: a new therapeutic option for solid tumors. J Cancer Res Ther 2010;6:414-420.
4. Jang HJ, Lee JY, Lee DH, Kim WH, Hwang JH. Current and future clinical applications of high-intensity focused ultrasound (HIFU) for pancreatic cancer. Gut Liver 2010;4 Suppl 1:S57-S61.
5. Kennedy JE. High-intensity focused ultrasound in the treatment of solid tumours. Nat Rev Cancer 2005;5:321-327.
6. Al-Bataineh O, Jenne J, Huber P. Clinical and future applications of high intensity focused ultrasound in cancer. Cancer Treat Rev 2012;38:346-353.
7. Yuh EL, Shulman SG, Mehta SA, Xie J, Chen L, Frenkel V, et al. Delivery of systemic chemotherapeutic agent to tumors by using focused ultrasound: study in a murine model. Radiology 2005;234:431-437.
8. Dittmar KM, Xie J, Hunter F, Trimble C, Bur M, Frenkel V, et al. Pulsed high-intensity focused ultrasound enhances systemic administration of naked DNA in squamous cell carcinoma model: initial experience. Radiology 2005;235:541-546.
9. Kohler MO, Mougenot C, Quesson B, Enholm J, Le Bail B, Laurent C, et al. Volumetric HIFU ablation under 3D guidance of rapid MRI thermometry. Med Phys 2009;36:3521-3535.
10. Martin E, Jeanmonod D, Morel A, Zadicario E, Werner B. High-intensity focused ultrasound for noninvasive functional neurosurgery. Ann Neurol 2009;66:858-861.
11. Elias WJ, Huss D, Voss T, Loomba J, Khaled M, Zadicario E, et al. A pilot study of focused ultrasound thalamotomy for essential tremor. N Engl J Med 2013;369:640-648.
12. Farny CH, Holt RG, Roy RA. Temporal and spatial detection of HIFU-induced inertial and hot-vapor cavitation with a diagnostic ultrasound system. Ultrasound Med Biol 2009;35:603-615.
13. Hsieh CY, Probert Smith P, Mayia F, Ye G. An adaptive spectral estimation technique to detect cavitation in HIFU with high spatial resolution. Ultrasound Med Biol 2011;37:1134-1150.
14. Nandlall SD, Jackson E, Coussios CC. Real-time passive acoustic monitoring of HIFU-induced tissue damage. Ultrasound Med Biol 2011;37:922-934.
15. Venkatesan AM, Partanen A, Pulanic TK, Dreher MR, Fischer J, Zurawin RK, et al. Magnetic resonance imaging-guided volumetric ablation of symptomatic leiomyomata: correlation of imaging with histology. J Vasc Interv Radiol 2012;23:786-794.e4.
16. Civale J, Clarke R, Rivens I, ter Haar G. The use of a segmented transducer for rib sparing in HIFU treatments. Ultrasound Med Biol 2006;32:1753-1761.
17. Ziadloo A, Vaezy S. Real-time 3D image-guided HIFU therapy. Conf Proc IEEE Eng Med Biol Soc 2008;2008:4459-4462.
18. Haar GT, Coussios C. High intensity focused ultrasound: physical principles and devices. Int J Hyperthermia 2007;23:89-104.
19. Haar GT, Coussios C. High intensity focused ultrasound: past, present and future. Int J Hyperthermia 2007;23:85-87.
20. Hwang JH, Tu J, Brayman AA, Matula TJ, Crum LA. Correlation between inertial cavitation dose and endothelial cell damage in vivo. Ultrasound Med Biol 2006;32:1611-1619.
21. Tu J, Hwang JH, Matula TJ, Brayman AA, Crum LA. Intravascular inertial cavitation activity detection and quantification in vivo with optison. Ultrasound Med Biol 2006;32:1601-1609.
22. Tung YS, Choi JJ, Baseri B, Konofagou EE. Identifying the inertial cavitation threshold and skull effects in a vessel phantom using

focused ultrasound and microbubbles. Ultrasound Med Biol 2010;36:840-852.
23. Bland JM, Altman DG. Statistical methods for assessing agreement between two methods of clinical measurement. Lancet 1986;1:307-310.
24. Unsgard G, Solheim O, Lindseth F, Selbekk T. Intra-operative imaging with 3D ultrasound in neurosurgery. Acta Neurochir Suppl 2011;109:181-186.
25. Bax J, Cool D, Gardi L, Knight K, Smith D, Montreuil J, et al. Mechanically assisted 3D ultrasound guided prostate biopsy system. Med Phys 2008;35:5397-5410.